

# Dark state localization of quantum emitters in a cavity

T. Botzung,<sup>1</sup> D. Hagenmüller,<sup>1</sup> S. Schütz,<sup>1</sup> J. Dubail,<sup>2,1</sup> G. Pupillo,<sup>1,\*</sup> and J. Schachenmayer<sup>3,1,†</sup>

<sup>1</sup> *Université de Strasbourg and CNRS, ISIS (UMR 7006) and icFRC, 67000 Strasbourg, France*

<sup>2</sup> *Université de Lorraine, CNRS, LPCT, F-54000 Nancy, France*

<sup>3</sup> *IPCMS (UMR 7504), CNRS, 67000 Strasbourg, France*

(Dated: April 30, 2022)

We study a disordered ensemble of quantum emitters collectively coupled to a lossless cavity mode. The latter is found to modify the localization properties of the “dark” eigenstates, which exhibit a novel character of being localized on multiple, non-contiguous sites. We denote such states as semi-localized and characterize them by means of standard localization measures. We show that those states can very efficiently contribute to coherent energy transport. Our work underlines the important role of dark states in systems with strong light-matter coupling.

When quantum emitters and a cavity mode coherently exchange energy at a rate faster than their decay, hybrid light-matter states play an important role [1–3]. Such polaritonic states are superpositions composed of “bright” emitter modes and cavity photons, while the numerous remaining emitter states have no photon contribution, i.e. they remain “dark”. Collective strong light-matter coupling has been intensively pursued in atomic [4–6] and condensed matter physics [7–12]. For example, polaritonic quasi-particles have been demonstrated to undergo Bose-Einstein condensation [13–18] and superfluidity [19–22] in laser-driven experiments. In contrast, strong coupling has been recently explored as a tool to engineer fundamental properties of matter, e.g. the critical temperature of superconductors [23, 24] or chemical reaction rates [25–32], without any external drive. Much interest is currently raised by the possibility of modifying energy [33–40] and charge [40–43] transport.

For transport, disorder plays a crucial role. It is well studied that coherent transport can be inhibited due to Anderson localization (AL) [44]. Here, an arbitrarily small disorder can lead to a localization of eigenstates in 1D and 2D [44, 45], while in 3D a metal-insulator transition driven by the disorder strength occurs [44, 46]. In this work, we study the fate of this coherent phenomenon in a cavity. While it is known that polaritonic states are largely unaffected by disorder [47] and can lead to a considerable enhancement of energy transmission [34–38, 40], the localization and transport properties of the dark states have remained largely unexplored. Moreover, disorder leads to a mixing of the bright with the dark states [48], which largely upends the usual description of light-matter coupling. Addressing these issues is expected to have important applications for the control of radiative energy transmission in mesoscopic systems.

In this work, we investigate a simple model for Anderson localization and coherent energy transport with  $N$  emitters collectively coupled to a cavity mode [Fig. 1(a)]. We focus on the impact of the cavity coupling on localized eigenstates, i.e. for a disorder strength much larger than the excitation hopping rate. We focus on the dark states of the system and find that they exhibit several

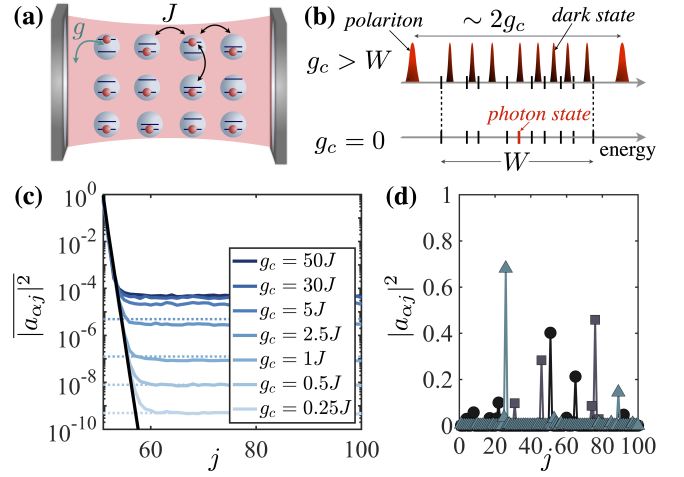


FIG. 1. (a) An excitation can hop with rate  $J$  on a disordered 3D lattice with  $N$  sites. Local transitions are coupled to a cavity with collective strength  $g_c \equiv g\sqrt{N}$ . (b) For  $g_c = J = 0$ , the  $N$  bare levels are randomly distributed in  $[-W/2, W/2]$ . For  $g_c > W$ , the spectrum contains two polaritons (splitting  $\sim 2g_c$ ) and  $N - 1$  dark states lying in between the bare levels. (c) Modification of the disorder-averaged weights of a dark eigenstate localized in the middle of a chain (1D for convenience) with  $N = 100$ , 2000 realizations,  $W = 25J$ . In addition to exponential localization at short distances (black line,  $g_c = 0$ ), a constant tail appears for  $g_c > 0$  (dashed lines: perturbative results). (d) Single disorder realization: three dark eigenstates are shown for  $g_c = 50J$  and  $W = 25J$ .

surprising features: for any strength of light-matter interactions, they acquire a squared amplitude  $\sim 1/N$ , on average, for arbitrary distances while remaining localized according to standard localization measures, such as the inverse participation ratio. However, we find that localization is distributed over two or more sites, which can be arbitrarily distant from one another. For large enough cavity coupling, they can be considered as hybridizations of a few localized states of the uncoupled system, and their energy lies in between those of the bare states. This results in semi-Poissonian statistics of the energy level spacings, which neither corresponds to that of a fully lo-

calized nor extended phase. We find that the dark states are responsible for a diffusive behavior, which is at odds with their localized nature. On average, the exponential decay of the excitation current with the system size for the uncoupled system is turned into an algebraic decay  $\sim 1/N$ , and can thus dominate over the  $\sim 1/N^2$  contribution expected from polaritonic states. This is in stark contrast with expectations from conventional polaritonic physics. Our results are based on both numerical calculations and analytical results for vanishing excitation hopping, and should be directly relevant to coherent transport experiments with semiconductors interacting with confined electromagnetic vacuum fields [49–51].

We consider a 3D cubic lattice of  $N$  two-level systems embedded in a cavity. The Hamiltonian ( $\hbar \equiv 1$ ) is  $\hat{H} = \hat{H}_0 + \hat{H}_I$ , with

$$\hat{H}_I = -J \sum_{\langle i,j \rangle} \hat{\sigma}_i^+ \hat{\sigma}_j^- + \sum_i w_i \hat{\sigma}_i^+ \hat{\sigma}_i^- + g \sum_i (\hat{a} \hat{\sigma}_i^+ + \hat{a}^\dagger \hat{\sigma}_i^-),$$

and  $\hat{H}_0 = \omega_c \hat{a}^\dagger \hat{a} + \omega_e \sum_i \hat{\sigma}_i^+ \hat{\sigma}_i^-$ . We restrict our discussion to a Hilbert space with a single excitation, i.e.  $\sum_i \hat{\sigma}_i^+ \hat{\sigma}_i^- + \hat{a}^\dagger \hat{a} = 1$ . Then, there are  $N + 1$  basis states,  $|\mathbf{i}, 0\rangle$ ,  $|G, 1\rangle$ , denoting states with an excitation on site  $\mathbf{i}$ , or in the cavity, respectively. Considering also the state without excitation,  $|G, 0\rangle$ , the spin lowering and photon annihilation operators are defined as  $\hat{\sigma}_i^- = |G, 0\rangle \langle \mathbf{i}, 0|$  and  $\hat{a} = |G, 0\rangle \langle G, 1|$ . In all numerical calculations, we consider the cavity mode (frequency  $\omega_c$ ) in resonance with the average emitter transition ( $\omega_e$ ), i.e.  $\delta \equiv \omega_e - \omega_c = 0$ . The first term in  $\hat{H}_I$  governs hopping (with rate  $J$ ) between nearest neighbor sites, indicated by the notation  $\langle \mathbf{i}, \mathbf{j} \rangle$ . Assuming periodic boundaries, this term is diagonalized by introducing the operators  $\hat{b}_{\mathbf{q}} = \sum_i \exp(-i\mathbf{q} \cdot \mathbf{i}) \hat{\sigma}_i^- / \sqrt{N}$ . The second term contains on-site disorder, with  $w_i$  random variables uniformly distributed in  $[-W/2, W/2]$ . The third term describes the Tavis-Cummings emitter-cavity coupling [1] with local strengths  $g$ . This term can be written in the form  $g_c(\hat{a} \hat{b}_0^\dagger + \hat{a}^\dagger \hat{b}_0)$  with the collective strength  $g_c = g\sqrt{N}$ , and couples the symmetric bright mode  $\hat{b}_{\mathbf{q}=0}$  to cavity photons. Importantly,  $g$  decreases with the cavity-mode volume  $V$  as  $g \sim 1/\sqrt{V}$  [52] and  $g_c$  thus remains independent of  $N$  for a fixed density  $N/V$ .

In the absence of disorder ( $W = 0$ ),  $\hat{H}_I$  has two polariton eigenstates  $|\psi_\pm\rangle = (\hat{b}_{\mathbf{q}=0}^\dagger \pm \hat{a}^\dagger)/\sqrt{2} |G, 0\rangle$  with energies  $E_\pm = \pm g_c$ , as well as  $N - 1$  uncoupled dark states  $|\psi_{\alpha \neq \pm}\rangle = \hat{b}_{\mathbf{q} \neq 0}^\dagger |G, 0\rangle$  with vanishing photon weight,  $\langle G, 1 | \psi_{\alpha \neq \pm} \rangle = 0$ . Finite disorder ( $W \neq 0$ ) leads to a coupling between the bright and the dark states since the second term in  $\hat{H}_I$  is non-diagonal in quasi-momentum space. The dark eigenstates therefore acquire a small photonic weight  $\langle G, 1 | \psi_{\alpha \neq \pm} \rangle \sim 1/N$  [53], and can be thought of as “grey” states. In the following we are interested in the modification of the emitter part of the system, and define the normalized emitter amplitudes as

$$a_{\alpha j} \equiv \langle \mathbf{j}, 0 | \psi_{\alpha \neq \pm} \rangle / \sqrt{\mathcal{N}_\alpha} \text{ with } \mathcal{N}_\alpha = 1 - |\langle G, 1 | \psi_\alpha \rangle|^2.$$

For  $g_c = 0$ ,  $\hat{H}$  corresponds to a usual Anderson model, displaying a  $W$ -dependent mobility edge that determines a metal-insulator transition at  $W_c \simeq 16.5J$  (for energy states lying in the middle of the band) [54–57]. While for  $W \ll W_c$  the eigenstates  $|\psi_\alpha\rangle$  resemble extended Bloch states, they are localized around given sites for  $W > W_c$ , e.g.  $|a_{\alpha j}|^2 \propto e^{-|i-j|/\xi}$  for a state localized on site  $\mathbf{i}$ , with  $\xi$  a  $W/J$ -dependent localization length. In the following, we investigate the case  $g_c, W \neq 0$ , and focus on spectral and transport properties of the Anderson insulator for strong collective light-matter couplings  $g_c > W > W_c$ .

The modification of Anderson localization in a cavity can be understood by first considering the eigenstates of  $\hat{H}$  for  $J = 0$ , in which case the spatial dimensionality becomes irrelevant. In second-order perturbation theory, a trivially localized eigenstate on site  $\mathbf{i}$ ,  $|\mathbf{i}, 0\rangle$ , for  $g_c = 0$  acquires an amplitude on site  $\mathbf{j} \neq \mathbf{i}$  via the cavity,  $b_{i \neq j} \equiv g^2 / [(w_j - w_i)(w_i + \delta)]$ , valid for configurations with  $g^2 \ll (w_j - w_i)(w_i + \delta)$ . A lower bound for the squared amplitude of perturbed localized states is thus  $|b_{i \neq j}|^2 \geq 4g_c^4 / (N^2 W^4)$ , setting  $\delta = 0$ . We find that the averaged value over disorder realizations (keeping only the finite part of the averaging integral) is  $|b_{i \neq j}|^2 = 4g_c^4 (4 - 2 \log(4)) / (N W^4)$  for large  $N$ . In Fig. 1(c) we show numerically that also for finite  $J \ll W$  the weights of an eigenstate localized in the center of a 3D cube, (logarithmically) averaged over disorder realizations, maintains an exponentially localized profile at short distances, followed by a constant tail rising with  $g_c$ . The tails are consistent with our perturbative result for small  $g$  (dashed lines) and saturate for strong couplings  $g_c > W > J$ . Note that a similar behavior was reported for dissipative couplings to a common reservoir [58, 59].

For strong coupling ( $g_c > W > J$ ), two polaritonic states  $|\psi_\pm\rangle$  with  $|\langle G, 1 | \psi_\pm \rangle|^2 \approx 0.5$  and separated by a splitting  $\sim 2g_c$  (only slightly modified by disorder) emerge from the band of width  $W$ . We find that the energies of the  $N - 1$  dark states lie in between the  $N$  bare ( $g_c = 0$ ) levels, which can be seen as a simple consequence of the “arrowhead” matrix shape of the single-excitation Hamiltonian for  $J = 0$  [60] [see Fig. 1(b)]. The strong cavity coupling leads to a hybridization between the bare levels that are close in energy, but not necessarily in real space. For a single disorder realization, the dark states appear strongly localized at multiple sites [see Fig. 1(d)]. We term this behavior as “semi-localization”.

Information about the spatial localization of the dark eigenstates with energy  $E_\alpha$  is given by the inverse participation ratio (IPR),  $\text{IPR}(E_\alpha) = \sum_{i=1}^N |a_{\alpha i}|^4$ . A finite, size-independent IPR indicates a localized eigenstate, while an IPR scaling as  $1/N \rightarrow 0$  indicates an extended one. Initializing the system in the state  $|\mathbf{i}, 0\rangle$ , the infinite-time-averaged probability to find an excitation at site  $\mathbf{j}$  is  $\Pi_{ij} = \lim_{T \rightarrow \infty} \int_0^T dt P_{ij}(t) / T$ , with

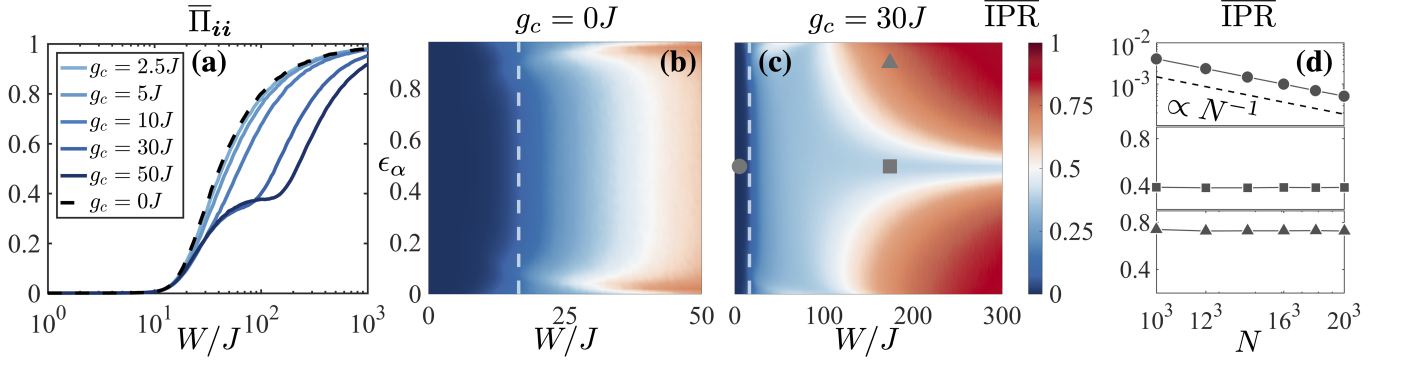


FIG. 2. **(a)** Disorder-averaged return probability  $\bar{\Pi}_{ii}$  as a function of  $W/J$  (for the central site  $i$  of a  $N = 15^3$  cube, mean emitter splitting on resonance with cavity,  $\delta = 0$ ). For strong-couplings  $g_c > W > W_c$ , a plateau ( $\bar{\Pi}_{ii} \simeq 0.4$ ) indicates a “semi-localized” regime. **(b-c)** Disorder-averaged inverse participation ratio  $\overline{\text{IPR}}(\epsilon_\alpha)$  as a function of  $W/J$  and the renormalized dark state energy  $\epsilon_\alpha$  (bins of widths 0.02,  $\sim 100$  realizations, white dashed line:  $W = W_c$ ). **(b)**  $g_c = 0$  (no cavity); **(c)**  $g_c = 30J$  (larger  $W/J$ -scale), showing an extended area with  $\overline{\text{IPR}}(\epsilon_\alpha) \simeq 0.4$ . **(d)** Finite-size scaling of  $\overline{\text{IPR}}(\epsilon_\alpha)$  for the parameters corresponding to the symbols in **(c)**. Square ( $W = 5J$ ,  $\epsilon_\alpha = 0.5$ ); circle ( $W = 175J$ ,  $\epsilon_\alpha = 0.5$ ); triangle ( $W = 175J$ ,  $\epsilon_\alpha = 0.9$ ).

$P_{ij}(t) \equiv |\langle j, 0 | \phi(t) \rangle|^2$  and  $|\phi(t)\rangle = e^{-i\hat{H}t} |i, 0\rangle$ . The IPR is connected to the return probability  $\Pi_{ii}$  by  $\sum_i \Pi_{ii} = \sum_\alpha \text{IPR}(E_\alpha) \mathcal{N}_\alpha^2$ . The  $\text{IPR}(E_\alpha)$  can thus be interpreted as the contribution of a given eigenstate to  $\sum_i \Pi_{ii}$ .

In Fig. 2(a), we compute numerically the disorder average of  $\Pi_{ii}$ ,  $\bar{\Pi}_{ii}$ , for the central site of a cubic lattice ( $N = 15^3$ ). For  $g_c = 0$  (dashed line),  $\bar{\Pi}_{ii}$  increases from 0 (extended phase) to 1 (localized phase) upon increasing the disorder strength  $W/J$ . Remarkably, we find that  $\bar{\Pi}_{ii}$  exhibits a plateau  $\simeq 0.4$  for  $g_c > W > J$ , which persists up to large disorder strengths ( $W \sim 100J$  for  $g_c = 50J$ ).

The disorder-averaged IPR,  $\overline{\text{IPR}}(E_\alpha)$ , is shown in Figs. 2(b-c) as a function of  $W/J$  for the Anderson model ( $g_c = 0$ ) and with a cavity coupling  $g_c = 30J$ . As we only focus on the dark states (in the band of width  $W$ ), we use a dimensionless, renormalized energy scale  $\epsilon_\alpha = (E_\alpha - W/2)/W$  with  $\epsilon_\alpha \in [0, 1]$ . For each disorder realization, we bin the different levels into groups with equal energy width and then average over realizations in each bin. Figure 2(b) shows the emergence of localized states upon increasing  $W/J$ , starting from the edges of the spectrum. A strong cavity coupling [Fig. 2(c)] leads to *three* distinct regimes: i) a delocalized region [ $\overline{\text{IPR}}(\epsilon_\alpha) \sim 0$  for  $W \lesssim W_c$ ]; ii) a fully localized region [ $\overline{\text{IPR}}(\epsilon_\alpha) \sim 1$  for  $W > g_c$ ]; and iii) an extended area with  $\overline{\text{IPR}}(\epsilon_\alpha) \sim 0.4$  where the dark states feature semi-localized characteristics consistent with the return probability and the results shown in Fig. 1(c). The persistence of semi-localized states in the vicinity of  $\epsilon_\alpha = 0.5$  ( $\delta = 0$ ) can be understood from the failure of perturbation theory, even for  $W \gg g_c$ . The energy separation between the two levels ( $i_0, j_0$ ) closest to  $\delta = 0$  is  $(w_{i_0} - w_{j_0}) \sim W/N$ . For them, the perturbation condition  $g_c^2 \ll W(w_{i_0}/j_0 + \delta)$  is violated for all  $W$  considered in Fig. 2(c), as they hybridize via the cavity.

Fig. 2(d), we analyze the finite size scaling of  $\overline{\text{IPR}}(\epsilon_\alpha)$

in the three regions [for parameters corresponding to the symbols in Fig. 2(c)]. We observe that the IPR of semi-localized states does not scale with the system size. These states exhibit the same behavior as in the fully localized region, only with a reduced value, which is consistent with states localized on multiple sites. In contrast,  $\overline{\text{IPR}}(\epsilon_\alpha) \propto 1/N$  for extended states.

Localization properties of eigenstates are also characterized by their level statistics [57]. Here, we numerically analyze the probability distribution function  $P(s_\alpha)$  for spacings between adjacent eigenenergies,  $s_\alpha = \epsilon_{\alpha+1} - \epsilon_\alpha$ . In Fig. 3(a), we plot  $P(s_\alpha)$  for eigenstates corresponding to the symbols in Fig. 2(c). While in the delocalized region ( $W \lesssim W_c$ )  $P(s_\alpha) = \frac{\pi}{2} s_\alpha \exp(-\frac{\pi}{4} s_\alpha^2)$  follows a Wigner-Dyson distribution, the fully localized phase is characterized by a Poissonian,  $P(s_\alpha) = \exp(-s_\alpha)$  [61]. Interestingly, we observe that the semi-

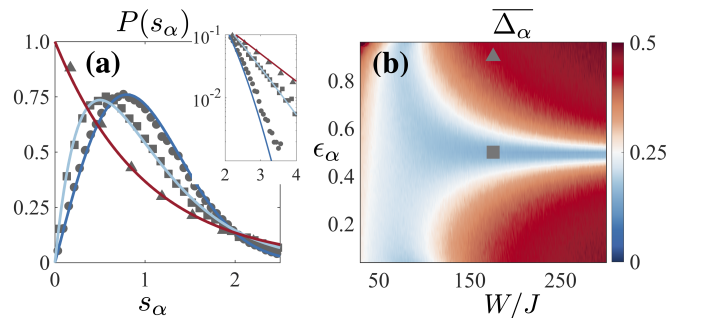


FIG. 3. **(a)** Comparison of numerically computed distributions  $P(s_\alpha)$  (symbols, parameters as in 2(c)) with analytical formulas (lines, see text). Wigner-Dyson distribution (dark blue); Poissonian distribution (red); Semi-Poissonian distribution (light blue). Inset: tails of the distributions on a logarithmic scale. **(b)** Numerically computed “dark state deviations”  $\bar{\Delta}_\alpha$  (see text) as a function of  $W/J$  for  $g_c = 30J$ .



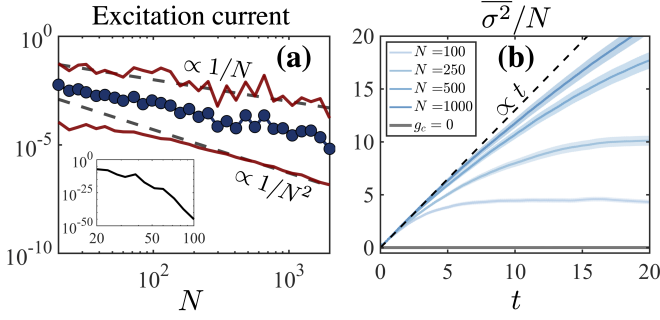


FIG. 4. **(a)** Excitation currents through a 1D chain as function of  $N$  (strong coupling,  $g_c = 30J$ ,  $W = 10J$ ,  $\gamma = 0.05J$ , see text). Shown are the mean ( $\bar{I}$ , blue circles) and maximum/minimum currents ( $I_{\max/\min}$ , red lines) of 100 disorder realizations. Dashed lines are guides to the eye for  $1/N$  and  $1/N^2$ . Inset:  $\bar{I} \propto e^{-N}$  for  $g_c = 0$ . **(b)** Disorder-averaged mean square displacement  $\bar{\sigma}^2/N$  (1D,  $g_c = 50J$ ,  $W = 30J$ , 200 realizations, see text). While absence of diffusion is found for  $g_c = 0$  ( $\bar{\sigma}^2/N \simeq 0$ , grey line, expected for 1D Anderson localization), diffusive dynamics,  $\bar{\sigma}^2 \propto t$ , occurs for  $g_c \gg W$ .

localized region features semi-Poissonian [62] statistics,  $P(s_\alpha) = 4s_\alpha \exp(-2s_\alpha)$ . We have checked that this behavior appears in the entire semi-localized region and is independent of the system size. The semi-Poissonian form can be simply understood for  $J = 0$ . Then, bare ( $g_c = 0$ ) levels follow a Poisson distribution. Since for strong coupling ( $g_c > W$ ) dark states lie in between the bare levels, we can model the dark state distribution as

$$P(s_\alpha) = \int dx dy \delta\left(s_\alpha - \frac{x+y}{2}\right) e^{-x} e^{-y} = 4s_\alpha e^{-2s_\alpha},$$

where we have assumed that the latter lie exactly at equal distance from the two closest bare levels. In order to check whether this property remains valid for  $J \neq 0$ , we also analyze numerically the disorder-averaged deviation  $\bar{\Delta}_\alpha = N\{E_\alpha - [(w_i + w_{i+1})/2]\}$  in Fig. 3(b), with  $w_i$  and  $w_{i+1}$  the closest bare levels immediately below and above the energy  $E_\alpha$ , respectively. While in the localized phase (triangle) the eigenenergies are found to be very close to the (fully localized) bare levels, they are much closer to  $(w_i + w_{i+1})/2$  in the semi-localized region (square), thereby confirming our simple argument above.

Finally, we investigate the role of semi-localized states on the transport and diffusion properties, in 1D for convenience. In Fig. 4(a), we analyze the excitation current flowing through the chain as a function of  $N$  (while keeping the emitter density constant). Starting in the state  $|G, 0\rangle$ , we numerically simulate evolution up to long times under a Lindblad master equation,  $d\hat{\rho}/dt = -i[\hat{H}_L, \hat{\rho}] + \sum_\eta \hat{\mathcal{L}}_\eta(\hat{\rho})$ , with  $\hat{\rho}$  the density matrix and two dissipative Lindblad processes adding and removing excitations on the first and last site, respectively. Here,  $\hat{\mathcal{L}}_\eta(\hat{\rho}) = -\{\hat{L}_\eta^\dagger \hat{L}_\eta, \hat{\rho}\} + 2\hat{L}_\eta \hat{\rho} \hat{L}_\eta^\dagger$  with  $\hat{L}_{\text{in}} = \sqrt{\gamma/2} \hat{\sigma}_1^\dagger$  and  $\hat{L}_{\text{out}} = \sqrt{\gamma/2} \hat{\sigma}_N$  (with  $\gamma$  a pump-

ing rate [35]). We find the dynamics to exhibit persistent small oscillations in the long-time limit (absence of dissipation), and thus average the normalized excitation current  $I \equiv \text{Tr}[\hat{\sigma}_N^\dagger \hat{\sigma}_N \hat{\rho}]$  at  $tJ = 4000$  over 100 disorder realizations. For  $g_c = 0$  we always find an exponentially suppressed current,  $\bar{I} \sim \exp(-N)$ , while  $\bar{I} \sim 1/N$  in the strong-coupling case ( $g_c = 30J$ ). Additionally, we also plot the maximum and minimum currents  $I_{\max}$  and  $I_{\min}$  out of the realizations. For large  $N$ ,  $I_{\min}$  decreases as  $\sim 1/N^2$  and exhibits only small fluctuations. Here, an “unlucky” disorder realization prohibits efficient dark-state transport, and the energy is flowing through the polaritonic states [35]. In contrast, the  $1/N$  decay of both  $I_{\max}$  and  $\bar{I}$  demonstrates the possibility of very efficient transport dominated by the dark states. These different scaling laws can be understood as follows: the polaritonic states feature homogeneous amplitudes  $a_{\pm,i} \sim 1/\sqrt{N}$ . Therefore, they contribute to the infinite-time averaged transmission probability,  $\Pi_{1N} \sim \sum_\alpha |a_{\alpha 1}|^2 |a_{\alpha N}|^2$ , with a term  $\sim 1/N^2$ . The  $1/N$  scaling of disorder-averaged dark state transport stems from the fact that the probability for an excitation to leave a site  $i$ ,  $1 - \bar{\Pi}_{ii} \sim 0.6$  is independent of  $N$  and evenly distributed over  $N - 1$  sites, therefore leading to a  $\Pi_{1N} \sim 1/N$  contribution.

In Fig. 4(b) we numerically analyze the diffusion properties in a 1D chain, after initializing the system in the state  $|\phi(t=0)\rangle = |N/2, 0\rangle$ . We show the time evolution of the disorder-averaged mean square displacement  $\bar{\sigma}^2 = \sum_j |i - j|^2 [1 - \bar{P}_{ii}(t)]$ . For  $g_c = 0$  and  $W = 30J$ , eigenstates are fully localized and diffusion is suppressed,  $\bar{\sigma}^2 \sim \text{cst}$ , while a diffusive behavior  $\lim_{N \rightarrow \infty} \bar{\sigma}^2 \propto t$  occurs in the strong coupling case ( $g_c = 50J$ ) up to finite size effects. Second order perturbation theory (Schrieffer-Wolff transformation [63]) leads to an effective *correlated* hopping model, with on-site energy dependent amplitude [64]. Diffusive behavior can be simply understood by computing  $1 - P_{ii}(t)$  using Fermi’s golden rule for large  $N$ . To first order in the effective hopping, this probability reads  $1 - P_{ii}(t) = 2\pi t g_c^4 / (N W w_i^2)$  for  $N/W \ll t \ll N w_i^2 W / (2\pi g_c^4)$ . An exact calculation for  $J = 0$  can be carried out by diagonalizing the arrowhead matrix Hamiltonian [53], showing that  $\bar{\sigma}^2 \propto t$  for all  $g_c$  and that this property solely originates from the contribution of dark states. The two polaritonic states lead to  $\bar{\sigma}^2 \sim t^4$  at short time ( $t \lesssim 1/g_c$ ) and generate small oscillations that are superimposed with the linear growth [65].

In conclusion, we have shown that Anderson localization can be strongly modified by coupling the disordered ensemble to a cavity. This is manifested by the emergence of dark states localized on multiple sites with energy spacings following semi-Poissonian statistics. These states are responsible for a diffusive behavior and an algebraic decay of energy transmission for strong light-matter couplings. It is an interesting prospect to investigate how dephasing and dissipation [58] can affect our results.

**Acknowledgements** — We are grateful to Denis Basko, Claudiu Genes, Nikolay Prokof'ev, and Antonello Scardicchio for stimulating discussions. This work was supported by the ANR - “ERA-NET QuantERA” - Projet “RouTe” (ANR-18-QUAN-0005-01), and LabEx NIE (“Nanostructures in Interaction with their Environment”) under contract ANR-11-LABX0058 NIE with funding managed by the French National Research Agency as part of the “Investments for the future program”. G. P. acknowledges support from the Institut Universitaire de France (IUF) and the University of Strasbourg Institute of Advanced Studies (USIAS).

\* pupillo@unistra.fr

† schachenmayer@unistra.fr

- [1] M. Tavis and F. W. Cummings, Exact Solution for an  $N$ -Molecule—Radiation-Field Hamiltonian, *Phys. Rev.* **170**, 379 (1968).
- [2] H. J. Kimble, Strong interactions of single atoms and photons in cavity QED, *Phys. Scr.* **T76**, 127 (1998).
- [3] J. M. Raimond, M. Brune, and S. Haroche, Manipulating quantum entanglement with atoms and photons in a cavity, *Rev. Mod. Phys.* **73**, 565 (2001).
- [4] Y. Kaluzny, P. Goy, M. Gross, J. M. Raimond, and S. Haroche, Observation of Self-Induced Rabi Oscillations in Two-Level Atoms Excited Inside a Resonant Cavity: The Ringing Regime of Superradiance, *Phys. Rev. Lett.* **51**, 1175 (1983).
- [5] M. G. Raizen, R. J. Thompson, R. J. Brecha, H. J. Kimble, and H. J. Carmichael, Normal-mode splitting and linewidth averaging for two-state atoms in an optical cavity, *Phys. Rev. Lett.* **63**, 240 (1989).
- [6] R. J. Thompson, G. Rempe, and H. J. Kimble, Observation of normal-mode splitting for an atom in an optical cavity, *Phys. Rev. Lett.* **68**, 1132 (1992).
- [7] C. Weisbuch, M. Nishioka, A. Ishikawa, and Y. Arakawa, Observation of the coupled exciton-photon mode splitting in a semiconductor quantum microcavity, *Phys. Rev. Lett.* **69**, 3314 (1992).
- [8] A. Imamoglu, R. J. Ram, S. Pau, and Y. Yamamoto, Nonequilibrium condensates and lasers without inversion: Exciton-polariton lasers, *Phys. Rev. A* **53**, 4250 (1996).
- [9] D. G. Lidzey, D. D. C. Bradley, M. S. Skolnick, T. Virgili, S. Walker, and D. M. Whittaker, Strong exciton-photon coupling in an organic semiconductor microcavity, *Nature* **395**, 53 (1998).
- [10] J. M. Fink, R. Bianchetti, M. Baur, M. Göppl, L. Steffen, S. Filipp, P. J. Leek, A. Blais, and A. Wallraff, Dressed Collective Qubit States and the Tavis-Cummings Model in Circuit QED, *Phys. Rev. Lett.* **103**, 083601 (2009).
- [11] Y. Kubo, F. R. Ong, P. Bertet, D. Vion, V. Jacques, D. Zheng, A. Dréau, J.-F. Roch, A. Auffeves, F. Jelezko, J. Wrachtrup, M. F. Barthe, P. Bergonzo, and D. Esteve, Strong Coupling of a Spin Ensemble to a Superconducting Resonator, *Phys. Rev. Lett.* **105**, 140502 (2010).
- [12] Y. Tabuchi, S. Ishino, T. Ishikawa, R. Yamazaki, K. Usami, and Y. Nakamura, Hybridizing Ferromagnetic Magnons and Microwave Photons in the Quantum Limit, *Phys. Rev. Lett.* **113**, 083603 (2014).
- [13] H. Deng, G. Weihs, C. Santori, J. Bloch, and Y. Yamamoto, Condensation of Semiconductor Microcavity Exciton Polaritons, *Science* **298**, 199 (2002).
- [14] J. Kasprzak, M. Richard, S. Kundermann, A. Baas, P. Jeambrun, J. M. J. Keeling, F. M. Marchetti, M. H. Szymańska, R. André, J. L. Staehli, V. Savona, P. B. Littlewood, B. Deveaud, and L. S. Dang, Bose-Einstein condensation of exciton polaritons, *Nature* **443**, 409 (2006).
- [15] R. Balili, V. Hartwell, D. Snoke, L. Pfeiffer, and K. West, Bose-Einstein Condensation of Microcavity Polaritons in a Trap, *Science* **316**, 1007 (2007).
- [16] J. Keeling, M. J. Bhaseen, and B. D. Simons, Collective Dynamics of Bose-Einstein Condensates in Optical Cavities, *Phys. Rev. Lett.* **105**, 043001 (2010).
- [17] H. Deng, H. Haug, and Y. Yamamoto, Exciton-polariton Bose-Einstein condensation, *Rev. Mod. Phys.* **82**, 1489 (2010).
- [18] D. Sanvitto and S. Kéna-Cohen, The road towards polaritonic devices, *Nat. Mater.* **15**, 1061 (2016).
- [19] A. Amo, D. Sanvitto, F. P. Laussy, D. Ballarini, E. d. Valle, M. D. Martin, A. Lemaître, J. Bloch, D. N. Krizhanovskii, M. S. Skolnick, C. Tejedor, and L. Viña, Collective fluid dynamics of a polariton condensate in a semiconductor microcavity, *Nature* **457**, 291 (2009).
- [20] A. Amo, J. Lefrère, S. Pigeon, C. Adrados, C. Ciuti, I. Carusotto, R. Houdré, E. Giacobino, and A. Bramati, Superfluidity of polaritons in semiconductor microcavities, *Nature Physics* **5**, 805 (2009).
- [21] I. Carusotto and C. Ciuti, Quantum fluids of light, *Rev. Mod. Phys.* **85**, 299 (2013).
- [22] G. Lerario, A. Fieramosca, F. Barachati, D. Ballarini, K. S. Daskalakis, L. Dominici, M. De Giorgi, S. A. Maier, G. Gigli, S. Kéna-Cohen, and D. Sanvitto, Room-temperature superfluidity in a polariton condensate, *Nature Physics* **13**, 837 (2017).
- [23] M. A. Sentef, M. Ruggenthaler, and A. Rubio, Cavity quantum-electrodynamical polaritonically enhanced electron-phonon coupling and its influence on superconductivity, *Science Advances* **4**, 10.1126/sciadv.aau6969 (2018).
- [24] A. Thomas, E. Devaux, K. Nagarajan, T. Chervy, M. Seidel, D. Hagenmüller, S. Schütz, J. Schachenmayer, C. Genet, G. Pupillo, and T. W. Ebbesen, Exploring Superconductivity under Strong Coupling with the Vacuum Electromagnetic Field, *arXiv* (2019), 1911.01459.
- [25] A. Thomas, L. Lethuillier-Karl, K. Nagarajan, R. M. A. Vergauwe, J. George, T. Chervy, A. Shalabney, E. Devaux, C. Genet, J. Moran, and T. W. Ebbesen, Tilting a ground-state reactivity landscape by vibrational strong coupling, *Science* **363**, 615 (2019).
- [26] S. Kéna-Cohen and J. Yuen-Zhou, Polariton Chemistry: Action in the Dark, *ACS Cent. Sci.* **5**, 386 (2019).
- [27] J. Lather, P. Bhatt, A. Thomas, T. W. Ebbesen, and J. George, Cavity Catalysis by Cooperative Vibrational Strong Coupling of Reactant and Solvent Molecules, *Angew. Chem. Int. Ed.* **58**, 10635 (2019).
- [28] A. Thomas, J. George, A. Shalabney, M. Dryzhakov, S. J. Varma, J. Moran, T. Chervy, X. Zhong, E. Devaux, C. Genet, J. A. Hutchison, and T. W. Ebbesen, Ground-State Chemical Reactivity under Vibrational Coupling to the Vacuum Electromagnetic Field, *Angew. Chem. Int. Ed.* **55**, 11462 (2016).
- [29] J. A. Hutchison, T. Schwartz, C. Genet, E. Devaux, and

- T. W. Ebbesen, Modifying Chemical Landscapes by Coupling to Vacuum Fields, *Angew. Chem. Int. Ed.* **51**, 1592 (2012).
- [30] F. Herrera and F. C. Spano, Cavity-Controlled Chemistry in Molecular Ensembles, *Phys. Rev. Lett.* **116**, 238301 (2016).
- [31] J. Galego, F. J. Garcia-Vidal, and J. Feist, Suppressing photochemical reactions with quantized light fields, *Nature Communications* **7**, 13841 (2016).
- [32] J. Flick, M. Ruggenthaler, H. Appel, and A. Rubio, Atoms and molecules in cavities, from weak to strong coupling in quantum-electrodynamics (QED) chemistry, *Proceedings of the National Academy of Sciences* **114**, 3026 (2017).
- [33] D. M. Coles, N. Somaschi, P. Michetti, C. Clark, P. G. Lagoudakis, P. G. Savvidis, and D. G. Lidzey, Polariton-mediated energy transfer between organic dyes in a strongly coupled optical microcavity, *Nat. Mater.* **13**, 712 (2014).
- [34] J. Feist and F. J. Garcia-Vidal, Extraordinary Exciton Conductance Induced by Strong Coupling, *Phys. Rev. Lett.* **114**, 196402 (2015).
- [35] J. Schachenmayer, C. Genes, E. Tignone, and G. Pupillo, Cavity-Enhanced Transport of Excitons, *Phys. Rev. Lett.* **114**, 196403 (2015).
- [36] X. Zhong, T. Chervy, L. Zhang, A. Thomas, J. George, C. Genet, J. A. Hutchison, and T. W. Ebbesen, Energy Transfer between Spatially Separated Entangled Molecules, *Angewandte Chemie International Edition* **56**, 9034 (2017).
- [37] G. Lerario, D. Ballarini, A. Fieramosca, A. Cannavale, A. Genco, F. Mangione, S. Gambino, L. Dominici, M. De Giorgi, G. Gigli, and D. Sanvitto, High-speed flow of interacting organic polaritons, *Light: Science & Applications* **6**, e16212 (2017).
- [38] M. Reitz, F. Mineo, and C. Genes, Energy transfer and correlations in cavity-embedded donor-acceptor configurations, *Sci. Rep.* **8**, 1 (2018).
- [39] M. Du, L. A. Martínez-Martínez, R. F. Ribeiro, Z. Hu, V. M. Menon, and J. Yuen-Zhou, Theory for polariton-assisted remote energy transfer, *Chem. Sci.* **9**, 6659 (2018).
- [40] C. Schäfer, M. Ruggenthaler, H. Appel, and A. Rubio, Modification of excitation and charge transfer in cavity quantum-electrodynamical chemistry, *Proceedings of the National Academy of Sciences* **116**, 4883 (2019).
- [41] E. Orgiu, J. George, J. A. Hutchison, E. Devaux, J. F. Dayen, B. Doudin, F. Stellacci, C. Genet, J. Schachenmayer, C. Genes, G. Pupillo, P. Samorì, and T. W. Ebbesen, Conductivity in organic semiconductors hybridized with the vacuum field, *Nat. Mater.* **14**, 1123 (2015).
- [42] D. Hagenmüller, J. Schachenmayer, S. Schütz, C. Genes, and G. Pupillo, Cavity-Enhanced Transport of Charge, *Phys. Rev. Lett.* **119**, 223601 (2017).
- [43] D. Hagenmüller, S. Schütz, J. Schachenmayer, C. Genes, and G. Pupillo, Cavity-assisted mesoscopic transport of fermions: Coherent and dissipative dynamics, *Phys. Rev. B* **97**, 205303 (2018).
- [44] F. Evers and A. D. Mirlin, Anderson transitions, *Rev. Mod. Phys.* **80**, 1355 (2008).
- [45] P. W. Anderson, Absence of Diffusion in Certain Random Lattices, *Phys. Rev.* **109**, 1492 (1958).
- [46] E. Abrahams, P. W. Anderson, D. C. Licciardello, and T. V. Ramakrishnan, Scaling Theory of Localization: Absence of Quantum Diffusion in Two Dimensions, *Phys. Rev. Lett.* **42**, 673 (1979).
- [47] R. Houdré, R. P. Stanley, and M. Illegems, Vacuum-field Rabi splitting in the presence of inhomogeneous broadening: Resolution of a homogeneous linewidth in an inhomogeneously broadened system, *Phys. Rev. A* **53**, 2711 (1996).
- [48] C. Gonzalez-Ballester, J. Feist, E. Gonzalo Badía, E. Moreno, and F. J. Garcia-Vidal, Uncoupled Dark States Can Inherit Polaritonic Properties, *Phys. Rev. Lett.* **117**, 156402 (2016).
- [49] P. Törmä and W. L. Barnes, Strong coupling between surface plasmon polaritons and emitters: a review, *Reports on Progress in Physics* **78**, 013901 (2014).
- [50] F. Cadiz, C. Robert, E. Courtade, M. Manca, L. Martinelli, T. Taniguchi, K. Watanabe, T. Amand, A. C. H. Rowe, D. Paget, B. Urbaszek, and X. Marie, Exciton diffusion in WSe<sub>2</sub> monolayers embedded in a Van der Waals heterostructure, *Applied Physics Letters* **112**, 152106 (2018).
- [51] S. S. Wang, X. J. Li, W. L. Zhang, and C. Y. Zheng, Transverse Anderson Localization of Exciton-Polaritons in Microcavities With Single-Layer WS<sub>2</sub>, *IEEE Journal of Selected Topics in Quantum Electronics* **25**, 1 (2019).
- [52] M. O. Scully and M. S. Zubairy, *Quantum Optics* (Cambridge University Press, 1997).
- [53] J. Dubail, T. Botzung, D. Hagenmüller, G. Pupillo, and J. Schachenmayer, *In preparation*.
- [54] A. MacKinnon and B. Kramer, One-Parameter Scaling of Localization Length and Conductance in Disordered Systems, *Phys. Rev. Lett.* **47**, 1546 (1981).
- [55] E. Hofstetter and M. Schreiber, Finite-Size Scaling and Critical Exponents. A New Approach and Its Application to Anderson Localisation, *Europhysics Letters (EPL)* **21**, 933 (1993).
- [56] B. I. Shklovskii, B. Shapiro, B. R. Sears, P. Lambrianides, and H. B. Shore, Statistics of spectra of disordered systems near the metal-insulator transition, *Phys. Rev. B* **47**, 11487 (1993).
- [57] I. K. Zharekeshev and B. Kramer, Scaling of level statistics at the disorder-induced metal-insulator transition, *Phys. Rev. B* **51**, 17239 (1995).
- [58] G. Celardo, A. Biella, L. Kaplan, and F. Borgonovi, Interplay of superradiance and disorder in the Anderson Model, *Fortschritte der Physik* **61**, 250 (2013).
- [59] A. Biella, F. Borgonovi, R. Kaiser, and G. L. Celardo, Subradiant hybrid states in the open 3D Anderson-Dicke model, *EPL* **103**, 57009 (2013).
- [60] D. O'Leary and G. Stewart, Computing the eigenvalues and eigenvectors of symmetric arrowhead matrices, *Journal of Computational Physics* **90**, 497 (1990).
- [61] F. Haake, *Quantum Signatures of Chaos* (Springer-Verlag, Berlin, Heidelberg, 2006).
- [62] E. B. Bogomolny, U. Gerland, and C. Schmit, Models of intermediate spectral statistics, *Phys. Rev. E* **59**, R1315 (1999).
- [63] G. Zhu, S. Schmidt, and J. Koch, Dispersive regime of the Jaynes-Cummings and Rabi lattice, *New Journal of Physics* **15**, 115002 (2013).
- [64] The effective hopping Hamiltonian (excluding reso-

nances) reads

$$\hat{H}' = \frac{1}{2} \sum_{i,j} \left( \frac{g^2}{w_i + \delta} + \frac{g^2}{w_j + \delta} \right) \hat{\sigma}_i^+ \hat{\sigma}_j^-.$$

It differs from other known models with long-range couplings, such as power-law hopping  $\sim J/|\mathbf{i}-\mathbf{j}|^\alpha$  with  $\alpha < d$  ( $d$  is the dimensionality). In this latter case, for random  $J$  all states are delocalized [66, 67], while for constant  $J$  and  $\alpha = 0$  essentially all states are localized [68]. Another model with random particle positions was studied in Refs. [69, 70], where wave functions were found to be localized algebraically for all  $\alpha$ .

- [65] T. Botzung, *Study of strongly correlated one-dimensional systems with long-range interactions*, Ph.D. thesis, University of Strasbourg, Ecole Doctorale des Sciences Chimiques (2019).
- [66] L. S. Levitov, Delocalization of vibrational modes caused

by electric dipole interaction, *Phys. Rev. Lett.* **64**, 547 (1990).

- [67] A. D. Mirlin, Y. V. Fyodorov, F.-M. Dittes, J. Quezada, and T. H. Seligman, Transition from localized to extended eigenstates in the ensemble of power-law random banded matrices, *Phys. Rev. E* **54**, 3221 (1996).
- [68] G. L. Celardo, R. Kaiser, and F. Borgonovi, Shielding and localization in the presence of long-range hopping, *Phys. Rev. B* **94**, 144206 (2016).
- [69] X. Deng, B. L. Altshuler, G. V. Shlyapnikov, and L. Santos, Quantum levy flights and multifractality of dipolar excitations in a random system, *Phys. Rev. Lett.* **117**, 020401 (2016).
- [70] X. Deng, V. E. Kravtsov, G. V. Shlyapnikov, and L. Santos, Duality in power-law localization in disordered one-dimensional systems, *Phys. Rev. Lett.* **120**, 110602 (2018).